Available online at www.sciencedirect.com

SCIENCE DIRECT

Developmental Biology 289 (2006) 115 – 126

DEVELOPMENTAL BIOLOGY

www.elsevier.com/locate/ydbio

Possible role of mouse poly(A) polymerase mGLD-2 during oocyte maturation

Tomoko Nakanishi [a], Haruka Kubota [a], Naoko Ishibashi [a], Satoshi Kumagai [a], Hiromi Watanabe [a], Misuzu Yamashita [a], Shin-ichi Kashiwabara [a], Kenji Miyado [b], Tadashi Baba [a,*]

[a] *Graduate School of Life and Environmental Sciences, University of Tsukuba, Tsukuba Science City, Ibaraki 305-8572, Japan*

[b] *Department of Reproductive Biology and Pathology, National Research Institute for Child Health and Development, Okura 2-10-1, Setagaya, Tokyo 157-8535, Japan*

Received for publication 16 February 2005, revised 24 September 2005, accepted 20 October 2005

Abstract

Cytoplasmic polyadenylation of mRNAs is involved in post-transcriptional regulation of genes, including translational activation. In addition to yeast Cid1 and Cid13 and mouse TPAP, GLD-2 has been recently identified as a cytoplasmic poly(A) polymerase in *Caenorhabditis elegans* and *Xenopus* oocytes. In this study, we have characterized mouse GLD-2, mGLD-2, in adult tissues, meiotically maturing oocytes, and NIH3T3 cultured cells. mGLD-2 was ubiquitously present in all tissues and cells tested. mGLD-2 was localized in the nucleus as well as in the cytoplasm of somatic, testicular, and cultured cells. Transfection of expression plasmids encoding mGLD-2 and the mutant proteins into NIH3T3 cells revealed that a 17-residue sequence in the N-terminal region of mGLD-2 probably acts as a localization signal required for the transport into the nucleus. Analysis of reverse transcriptase-polymerase chain reaction indicated the presence of mGLD-2 mRNA in the oocytes throughout meiotic maturation. However, 54-kDa mGLD-2 was found in the oocytes only at the metaphases I and II after germinal vesicle breakdown, presumably due to translational control. When mGLD-2 synthesis was artificially inhibited and enhanced by injection of double-stranded and polyadenylated RNAs into the germinal vesicle-stage oocytes, respectively, oocyte maturation was significantly arrested at the metaphase-I stage. These results suggest that mGLD-2 may act in the ooplasm on the progression of metaphase I to metaphase II during oocyte maturation.

Keywords: GLD-2; mRNA; Poly(A) tail; Cytoplasmic polyadenylation; Nuclear transport; Translational control; Oocyte maturation; Mouse oocytes

Introduction

Polyadenylation of mRNA precursors initially occurs in the nucleus of eukaryotic cells, and the polyadenylated mRNAs are then transported into the cytoplasm. The processing of the mRNA precursors at the 3′-end is one of the post-transcriptional gene regulations because the length of the poly(A) tail is implicated in various aspects of mRNA metabolism, including the transport of mRNAs into the cytoplasm, mRNA stability, and translational control of mRNAs (Sachs et al., 1997; Wickens et al., 1997). In particular, the lengthening, maintenance, and shortening of the poly(A) tails in the cell cytoplasm are essential for modulation of gametogenesis (Kashiwabara et al., 2000, 2002; Wang et al., 2002) and early embryonic development (Kuersten and Goodwin, 2003; Richter, 1999); for instance, meiotic maturation of *Xenopus* and mouse oocytes has been reported to require cytoplasmic polyadenylation of c-*mos* mRNA for synthesis of the Mos protein responsible for the stabilization and activation of maturation promoting factor MPF (Colledge et al., 1994; Gebauer et al., 1994; Hashimoto et al., 1994; Sheets et al., 1995).

In *Xenopus* oocytes, cytoplasmic polyadenylation is controlled by several core factors: CPEB (Hake et al., 1998; Mendez and Richter, 2001), CPSF (Bilger et al., 1994; Dickson et al., 1999), and maskin (Cao and Richter, 2002; Stebbins-Boaz et al., 1999) capable of binding to the cytoplasmic polyadenylation element UUUUA/UAU (CPE), to the polyadenylation hexanucleotide AAUAAA, and to both

* Corresponding author. Fax: +81 29 853 7196.
E-mail address: acroman@sakura.cc.tsukuba.ac.jp (T. Baba).

0012-1606/$ - see front matter © 2005 Elsevier Inc. All rights reserved.
doi:10.1016/j.ydbio.2005.10.017

CPEB and an mRNA cap structure (m^7GpppN)-binding protein, eIF4E, respectively. When Eg2, a member of the aurora Ser/Thr protein kinase family, phosphorylates the Ser-174 residue in CPEB, the interaction between the AAUAAA element and CPSF is presumably stabilized by phosphorylated CPEB, leading to the recruitment of poly(A) polymerase (PAP) to the 3′-end of mRNA (Mendez and Richter, 2001). In addition to the above core factors, two novel proteins essential for cytoplasmic polyadenylation have been recently identified: CPEB- and CPSF-binding protein symplekin and cytoplasmic PAP GLD-2 that act as scaffold and anchored proteins in the cytoplasmic polyadenylation machinery, respectively (Barnard et al., 2004). Thus, the molecular mechanism of cytoplasmic polyadenylation has been defined in *Xenopus* oocytes. However, little is known of the mechanism in the mammalian oocytes.

Despite the presence of the protein complex governing cytoplasmic polyadenylation, PAP is the sole enzyme capable of elongating poly(A) tail at the 3′-end of mRNA. Several cytoplasmic PAPs, Cid1 (Read et al., 2002; Wang et al., 2000), Cid13 (Read et al., 2002; Saitoh et al., 2002), and GLD-2 (Barnard et al., 2004; Wang et al., 2002), which are structurally distinguishable from nuclear PAP (Martin et al., 2000, 2004; Raabe et al., 1991, 1994; Thuresson et al., 1994; Wahle, 1991; Zhao and Manley, 1996), have been characterized in yeast, *Caenorhabditis elegans*, and *Xenopus*. Yeast Cid13 participates in DNA replication and genome maintenance (Saitoh et al., 2002), while yeast Cid1 and *C. elegans* GLD-2 are involved in the cell cycle control such as the inhibition of mitosis and entry into meiosis (Kadyk and Kimble, 1998; Read et al., 2002; Wang et al., 2000). In mammalian cells, five PAPs have been identified: canonical PAP (PAPI and PAPII) (Raabe et al., 1991, 1994; Thuresson et al., 1994; Zhao and Manley, 1996), TPAP (Kashiwabara et al., 2000, 2002), neo-PAP/PAPγ (Kyriakopoulou et al., 2001; Topalian et al., 2001), GLD-2 (Kwak et al., 2004; Rouhana et al., 2005; Wang et al., 2002), and nuclear-encoded mitochondrial PAP, mitoPAP (Tomecki et al., 2004). These mammalian PAPs except TPAP, GLD-2, and mitoPAP are exclusively localized in the nucleus. Only TPAP in spermatogenic cells (Kashiwabara et al., 2000, 2002) is characterized as a cytoplasmic PAP among mammalian PAPs, and the subcellular localization of GLD-2 in mammalian cells has not yet been ascertained. Moreover, the biological roles of mammalian PAPs except TPAP are still uncertain, although these PAPs all exhibit the polyadenylation activity.

In this study, we have demonstrated that mouse GLD-2, termed mGLD-2, is a PAP localized in both cytoplasm and nucleus of somatic, testicular, and cultured cells. However, mGLD-2 is synthesized in the cytoplasm of mouse oocytes following germinal vesicle breakdown (GVBD) because the GLD-2 mRNA is under translational control at the early stages of oocyte maturation. Both impaired and enhanced productions of mGLD-2 significantly result in the oocyte arrest at the metaphase-I stage. Thus, mGLD-2 may function in the progression of metaphase I to metaphase II during oocyte maturation.

Materials and methods

Polymerase chain reaction (PCR)

An unfertilized mouse oocyte cDNA library was prepared from total cellular RNA of metaphase II-arrested mouse oocytes using a HybriZAP-2.1 XR library construction kit (Stratagene). A DNA fragment encoding mGLD-2 (GenBank/EBI accession number NM_133905) was amplified by PCR using the cDNA library as a template. The following oligonucleotides were used as primers: SEP5 (5′-TTCCATGGTCCCAAACTCAATTTTGGGT-3′) and SEP19 (5′-AAGTCGACTTATCTTTTCAGGGTAGCAGC-3′). Reactions were performed in a 50-μl mixture containing 10 mM Tris/HCl, pH 8.8, 50 mM KCl, 1.5 mM $MgCl_2$, 0.1% Triton X-100, 0.2 mM each of dATP, dCTP, dGTP, and dTTP, 1 μM each of primers, template cDNA, and 2 units of *Taq* DNA polymerase (Nippon Gene, Toyama, Japan). The reaction program consisted of 35 cycles of 94°C for 60 s, 60°C for 60 s, and 72°C for 120 s. The PCR product was then introduced into a pTV119N vector (Takara Bio Inc., Shiga, Japan) at *Nco*I and *Sal*I sites. DNA fragments were also PCR-amplified from a mouse testis cDNA library (Kashiwabara et al., 1990) using following oligonucleotides as primers: SEP50, 5′-TCGGCCCTTCGGCGTGGACG-3′; SEP12, 5′-TGTCGACTGTAGGCCTACAAGAAGTT-3′; SEP11, 5′-TGGATCCA-GATCTGAACAGTGTGCTGC-3′; SEP53, 5′-CACGATTAGGTTCCGAT-CAG-3′; SEP7, 5′-AAGTCGACACTTGCTTGCTGCTGACAA-3′; SEP46, 5′-CAGAGCTGTGCATGAGAAGC-3′; SEP18, 5′-AGCAACCTCCAGAG-TCTATC-3′. Nucleotide sequencing was carried out using an ABI Prism 310 genetic analyzer.

Northern blot analysis

Total cellular RNAs were extracted from various tissues and cells using Isogen (Nippon Gene), as described previously (Kashiwabara et al., 2000). The RNA samples were glyoxylated, separated by electrophoresis on 1.2% agarose gels, and transferred onto Hybond-N^+ nylon membranes (Amersham Biosciences). The blots were probed by ^{32}P-labeled DNA fragments and analyzed by autoradiography or a BAS-1800II Bio-Image Analyzer (Fuji Photo Film, Tokyo, Japan).

Preparation of cytoplasmic and nuclear extracts

Mouse tissues (0.5 g each) were homogenized at 4°C in 5 ml of 10 mM HEPES/KOH, pH 7.4, containing 15 mM KCl, 1 mM EDTA, 0.25 M sucrose, 0.5 mM dithiothreitol, 0.5 mM phenylmethanesulfonyl fluoride, pepstatin A (1 μg/ml), leupeptin (1 μg/ml), and 1 mM benzamidine with a Teflon-glass homogenizer at 800 rpm (5 strokes). The homogenate was centrifuged at 2500 × *g* for 10 min at 4°C. The supernatant was further centrifuged at 15,000 × *g* for 20 min, and the resulting supernatant was used as "cytoplasmic extract." The precipitate obtained by the first centrifugation was suspended in the above buffer (5 ml), overlaid onto the same buffer (5 ml) containing 0.5 M sucrose, and centrifuged at 2500 × *g* for 10 min at 4°C. This treatment was repeated three times, and the remaining pellet was resuspended in the same buffer (1 ml) containing 0.5 M NaCl, mixed gently for 1 h, and then centrifuged at 90,000 × *g* for 1 h at 4°C. The supernatant solution was used as "nuclear extract." Nuclear and cytoplasmic extracts of NIH3T3 cells were prepared by using a PARIS kit (Ambion) according to the manufacturer's protocol. Protein concentration was determined using a Coomassie protein assay reagent kit (Pierce).

Antibodies

Two DNA fragments encoding the C-terminal 149- and 62-residue sequences of mGLD-2 were PCR-amplified, introduced into pET-23d (Novagen) and pGEX-4T-1 (Amersham Biosciences), respectively, and expressed in *Escherichia coli* BL21 (DE3). The 149-residue protein tagged with six His was purified on an Ni-NTA His column (Novagen), emulsified with Freund's complete adjuvant (Difco Laboratories), and injected intradermally into female New Zealand White rabbits (SLC Inc., Shizuoka, Japan). Following fractionation of antisera with ammonium sulfate (0–40% saturation), anti-mGLD-2

antibody was affinity-purified on a Sepharose 4B column that had been coupled with the above 62-residue protein fused to glutathione *S*-transferase, as described previously (Honda et al., 2002). Antibodies against β-tubulin (T5293), FLAG, histone deacetylase 2 (HDAC2, H-54), and hemagglutinin (HA) were purchased from Sigma (St. Louis, MO), Stratagene (La Jolla, CA), Santa Cruz Biotechnology (Santa Cruz, CA), and Roche Diagnostics (Indianapolis, IN), respectively.

Immunoblot analysis

Proteins were separated by SDS-polyacrylamide gel electrophoresis (PAGE) and transferred onto Immobilon-P polyvinylidene difluoride membranes (Millipore). After blocking with 2% skim milk, the blots were probed by primary antibodies and then incubated with secondary antibodies conjugated with horseradish peroxidase (Jackson Immunoresearch Laboratories). The immunoreactive proteins were visualized by an ECL Western blotting detection kit (Amersham Biosciences), as described (Nishimura et al., 2004).

Measurement of enzyme activity

Recombinant proteins were produced in vitro by using a TNT Quick Coupled Transcription/Translation system (Promega), as described previously (Kashiwabara et al., 2000). Poly(A) polymerase activity was determined by measuring incorporation of AMP from [α-^{32}P]ATP (400 Ci/mmol, Amersham Biosciences) into oligo(A)$_{12}$ RNA primer in the presence of $MnCl_2$ (Kashiwabara et al., 2000; Zhao and Manley, 1996). The reaction mixture (50 μl) consisted of 50 mM Tris/HCl, pH 8.3, 7% glycerol, 0.3% polyvinyl alcohol, 40 mM KCl, 0.5 mM $MnCl_2$, 25 mM $(NH_4)_2SO_4$, 0.25 mM dithiothreitol, 0.1 mM [α-^{32}P]ATP (600 cpm/pmol), 2 μg oligo(A)$_{12}$, and an aliquot of in vitro translation product. After incubation at 30°C, aliquots (3 μl) were spotted onto Whatman DE-81 paper, dried, and washed five times with 0.1 M phosphate buffer, pH 7.0, and once with ethanol. Incorporation of ^{32}P-labeled AMP was then measured by liquid scintillation counting.

Cell culture

NIH3T3 cells were transfected with expression plasmids using a FuGENE 6 transfection reagent (Roche Diagnostics) and cultured in Dulbecco's modified Eagle's medium supplemented with 10% fetal bovine serum, 100 units/ml penicillin, and 0.1 mg/ml streptomycin at 37°C under 5% CO_2 in air. After 48-h incubation, cells were observed under an Olympus IX-70 epifluorescent microscope.

RNA synthesis in vitro

DNA fragments were introduced into a pcDNA3.1 vector, and the resulting plasmids were linearized by cutting with *Not*I. RNAs were synthesized by T7 polymerase using a RiboMAX large scale RNA production systems-T7 kit (Promega) and then polyadenylated by using a Poly(A) tailing kit (Ambion). The polyadenylated RNAs were extracted with phenol-chloroform, precipitated with ethanol, and dissolved in water. For preparation of double-stranded RNA (dsRNA), 628- and 650-bp DNA fragments derived from mGLD-2 and Mos cDNAs, respectively, were introduced into pBluscriptII SK or KS. The plasmids were linearized and used as templates for RNA synthesis as described above. The sense and antisense single-strand RNAs (4 μM each) were then mixed in 10 mM Tris/HCl buffer, pH 7.4, containing 0.1 mM EDTA, heated at 95°C for 5 min, and kept at room temperature for 16 h. Remaining single-strand RNA was digested with RNase T1 (2 U/μl) for 30 min at 37°C. dsRNA so obtained was dissolved in water and stored at −80°C.

Oocyte collection and microinjection

Fully grown, GV-stage oocytes were prepared from ovaries of 8-week-old ICR mice (SLC Japan) 46–48 h after intraperitoneal injection of pregnant mare's serum gonadotropin (Teikokuzoki Co., Tokyo, Japan), as described previously (Schultz et al., 1983). Cumulus cells attached with the oocytes were removed by pipetting. The oocytes were cultured in a 0.2-ml drop of a modified Krebs–Ringer bicarbonate solution (TYH medium) (Toyoda et al., 1971) containing 5% fetal bovine serum and 0.24 mM N^6,2′-*O*-dibutyryladenosine 3′5′-cyclic monophosphate (dbcAMP) (Sigma) at 37°C under 5% CO_2 in air. RNA samples (10 pl) were microinjected into the cytoplasm of the oocytes using a Femtojet constant flow system (Eppendorf). The oocytes were cultured in TYH medium containing 5% fetal bovine serum and 0.24 mM dbcAMP, washed thoroughly with the TYH medium free from dbcAMP, and then cultured in the same medium. All animal experiments were carried out according to the *Guide for the Care and Use of Laboratory Animals* in University of Tsukuba.

Semi-quantitative PCR

First-strand cDNA was synthesized from total RNA of 10 oocytes using a full 3′-RACE kit (Takara Bio) according to the manufacturer's protocol, as described previously (Ohmura et al., 1999). PCR was carried out using the first-strand cDNA as a template. The reaction program for mGLD-2 and PAPII consisted of 32 cycles of 94°C for 30 s, 60°C for 30 s, and 72°C for 40 s (29 cycles for Mos and glyceraldehyde-3-phosphate dehydrogenase, G3PDH). The numbers of the reaction cycles were determined on the basis of linear regions of the semi-log plots for the amount of PCR-amplified products. The following oligonucleotides were used as primers: SEP5 (5′-TTCCATGGTCCCAAACTCAATTTTGGGT-3′) and SEP7 (5′-AAGTCGACACTTGCTTGCTGCTGACAA-3′) for mGLD-2; MOS5 (5′-ACTCGAGTTCGTAACTTTATTTCC-3′) and MOS6 (5′-TCAGTGACTTCGGCTGCTCC-3′) for Mos; G3PP1 (5′-AGTGGAGATTGTTGCCATCAACGAC-3′) and G3PP2 (5′-GGGAGTTGCTGTTGAAGTCGCAGGA-3′) for G3PDH; PPP1 (5′-GGAATTCAGACGATGCCGTTTCCAGT-3′) and PPP2 (5′-GGAATTCCGTAGGTCCAAATCTTCTGG-3′) for PAPII. The PCR products were separated by agarose gel electrophoresis and quantified by a ChemiDoc XRS densitometer (Bio-Rad) using a Quantity One software.

Immunohistochemistry

Oocytes were fixed in phosphate-buffered saline (PBS) containing 2% paraformaldehyde for 30 min and in PBS containing 2% formaldehyde for 1 h, treated with 1% Triton X-100 in PBS for 15 min, and blocked with PBS containing 3% goat serum and 0.05% Tween-20 overnight. The oocytes were then incubated with primary antibodies in the blocking solution for 3 h, washed with PBS, and reacted with secondary antibodies conjugated with Alexa Fluor 488 or 568 (Molecular Probes, Eugene, OR), as described previously (Kim et al., 2004). The nuclei of the oocytes were stained with Hoechst 33342. After washing with PBS containing 0.05% Tween-20, the oocytes were observed using an Olympus IX-70 inverted microscope equipped with a SPOT RT camera (Diagnostic Instruments). The 16-bit digital images were analyzed by using a Metamorph software.

PCR-based poly(A) test (PAT)

Lengths of mRNA poly(A) tails were measured by PAT assays as described previously (Rassa et al., 2000; Kashiwabara et al., 2002). Briefly, total RNA from 50 oocytes was ligated to a 32-mer RNA oligonucleotide, 5′-UACGCAUCAUACGCUGUGGCGUACCUUGUA-3′ (60 pmol) and reacted at 42°C for 50 min with SuperScript II reverse transcriptase (Invitrogen), using a PAT1 oligonucleotide, 5′-ACAAGGTACGCCACAGCGTATG-3′, as a primer. A portion of the reaction mixture was subjected to first round PCR using a set of PAT1 and a gene-specific primer listed below. Second round PCR was carried out using a nested set of primers, PAT2, 5′-GGCTCGAGGTACGCCACAGCGTATGATG-3′, and another gene-specific primer. The PCR reaction consisted of 20 cycles (30 cycles for the second round PCR) of 94°C for 30 s, 60°C for 30 s, and 72°C for 30 s. The DNA fragments were separated on agarose gels and stained with ethidium bromide. The gene-specific primers used for first and second round PCRs were as follows: SEP11, 5′-TGGATCCAGATCTGAACAGTGTGCTGC-3′, and SEP44, 5′-TGCCTTTGAGAGCTGCTACC-3′, for mGLD-2; CYB4, 5′-GGCTTCATTCATAGTAGCTC-3′, and CYB3, 5′-TCCTGTCTTGTAATGCCACCTG-3′, for cyclin B1; MOS10, 5′-AACATCATCCAGAGCTGCTG-3′, and MOS9, 5′-

ACTCCATCGAGCCGATTGTAG-3′, for Mos; CAT2, 5′-TTGGACAGTATACCAGTTGC-3′, and CAT1, 5′-AGGTGACAGCATTGCTTCTG-3′, for β-catenin; ACT2, 5′-AGGTGACAGCATTGCTTCTG-3′, and ACT1, 5′-TTTCTGAATGGCCCAGGTCTG-3′, for β-actin.

Results

Although the outlines of mammalian GLD-2, including mGLD-2, have been reported (Kwak et al., 2004; Rouhana et al., 2005; Wang et al., 2002), the details remain to be clarified. We thus amplified a DNA fragment carrying the entire protein-coding region of mGLD-2 by PCR using an unfertilized mouse oocyte cDNA library as a template. The nucleotide sequence of the amplified DNA fragment indicated that several sequence elements required for polyadenylation activity are conserved in mGLD-2: three Asp residues and putative ATP-interacting residues necessary for binding to two divalent cations and substrate ATP involved in the enzymatic catalysis, respectively (Fig. 1A). As compared with mouse nuclear PAPII (Raabe et al., 1991; Zhao and Manley, 1996), mGLD2 possessed an approximately 120-residue extra sequence at the N-terminus and lacked a C-terminal sequence of almost 330 residues containing the RNA-binding and Ser/Thr-rich domains, and two bipartite nuclear localization signals (NLSs). A sequence similar to the cyclin-recognition motif (CRM) in PAPII (Bond et al., 2000) was also present at residues 468–471 in the C-terminal region of mGLD-2. Noteworthy was that the consensus sequences for bipartite NLS and leucine zipper motif are present at residues 76–92 and 142–163 in the N-terminal region of mGLD-2, respectively (Fig. 1A). The catalytic and central domains of mGLD-2 shared high degrees of sequence identities (74 and 94%) with those of *Xenopus* and human GLD-2, respectively, whereas the mouse sequence was highly divergent to the *C. elegans* sequence (39% identity).

Northern blot analysis indicated that two forms of mGLD-2 mRNA with sizes of 3.5 and 2.3 kb are present in all mouse tissues tested (Fig. 1B). On the basis of the genomic DNA sequence of mGLD-2 on the NCBI Genomic Biology database (http://www.ncbi.nlm.nih.gov/Genomes/), three DNA fragments were PCR-amplified from a mouse testicular cDNA library using different sets of oligonucleotide primers. Sequence analysis of the amplified fragments indicated that the protein-coding region of the 3.5-kb form (long form) of mGLD-2 mRNA is identical to that of the 2.3-kb form (short form) of mRNA (GenBank/EMBL accession number NM_133905). These two mRNAs are distinguished by the length of the 3′-untranslated region encoded by the same exon (15th exon) of the mGLD-2 gene. Indeed, only 3.5-kb mRNA signal was detected when a DNA fragment (probe 2) carrying the 378-bp 3′-untranslated region of the longer mRNA form was used as a probe. These data are consistent with the recent finding that two mRNA forms of GLD-2, which contain the same protein-coding region, but differ in the length of the 3′-untranslated region, are present in *Xenopus* oocytes and mouse and human tissues (Rouhana et al., 2005). As expected by the expression pattern, 54-kDa mGLD-2 was found in all tissues, despite that the protein level was relatively low in the brain, heart, and spleen (Fig. 1C). These data suggest ubiquitous expression of the mGLD-2 gene in the mouse tissues. It should be noted that a 51-kDa protein immunoreactive with affinity-purified anti-mGLD-2 antibody was also present in all mouse tissues (Fig. 1C). The 51-kDa protein was abundantly present in the brain and relatively rich in the testis and ovary. Because 54-kDa mGLD-2 in ovarian protein extracts was solely immunodepleted by antibody against the N-terminal 99-residue polypeptide of mGLD-2, the 51-kDa protein nonspecifically immunoreacted with affinity-purified anti-mGLD-2 antibody.

mGLD-2 was shown to exhibit a polyadenylation activity toward an artificial RNA substrate when an mRNA construct encoding mGLD-2 fused to RNA-binding protein MS2 was expressed in *Xenopus* oocytes (Kwak et al., 2004). In this study, we examined nonspecific polyadenylation activity of mGLD-2 under assay conditions where the enzyme affinity toward RNA primers increased independently of the polyadenylation hexanucleotide, AAUAAA, and CPSF (Wahle, 1991). Recombinant mGLD-2 protein fused to a FLAG/HA tag, which migrated as a 56-kDa polypeptide on SDS-PAGE, was capable of transferring the AMP moiety from [α-^{32}P]ATP to oligo(A)$_{12}$ RNA primer (Fig. 2A). When one of the active-site Asp residues in mGLD-2 was point-mutated by Ala, the mutant protein, D215A, exhibited approximately 90% reduction in activity.

As described above, the subcellular localization of mammalian GLD-2 is still uncertain. Immunoblot analysis indicated that 54-kDa mGLD-2 is predominantly present in the nuclear fractions of liver, testis and NIH3T3 cells but is also localized at a low level in the cytoplasmic fractions (Fig. 3A). To ascertain the localization of mGLD-2 in the nucleus, five expression plasmids encoding fusion proteins between EGFP and mGLD-2, PAPII, or three mGLD-2 mutants (ΔN94, Δ73–94, and ΔC132) were constructed and expressed in NIH3T3 cells (Fig. 3B). Fluorescent microscopic analysis of the fusion proteins demonstrated the nuclear localization of EGFP/mGLD-2 and EGFP/PAPII (Fig. 3C). The EGFP/mGLD-2ΔC132 fusion protein was also present in the cell nucleus, whereas the cytoplasmic localization was obvious in the EGFP/mGLD-2ΔN94 and EGFP/mGLD-2Δ73–94 proteins. These data suggest that the bipartite NLS of mGLD-2 at residues 76–92 (Fig. 1A) is probably required for the transport into the nucleus because the EGFP/mGLD-2ΔN94 and EGFP/mGLD-2Δ73–94 proteins lack the NLS sequence among four EGFP/mGLD-2 fusion proteins tested (Fig. 3B).

C. elegans GLD-2 is a regulatory protein important for normal progression through meiotic prophase and for promotion of the entry into meiosis during gametogenesis (Kadyk and Kimble, 1998; Wang et al., 2002). We thus selected mouse oocyte as an experimental model to elucidate the functional role(s) of mGLD-2 during meiotic maturation. Two DNA fragments corresponding to the long form of mGLD-2 mRNA and both long and short forms (Fig. 1B) were amplified from total RNAs of the oocytes at GV through metaphase-II stages by reverse transcriptase (RT)-PCR (Fig. 4A). The mRNA level of the long form was apparently very low. When polyadenylation of two mGLD-2 mRNAs was examined by PAT assay, the

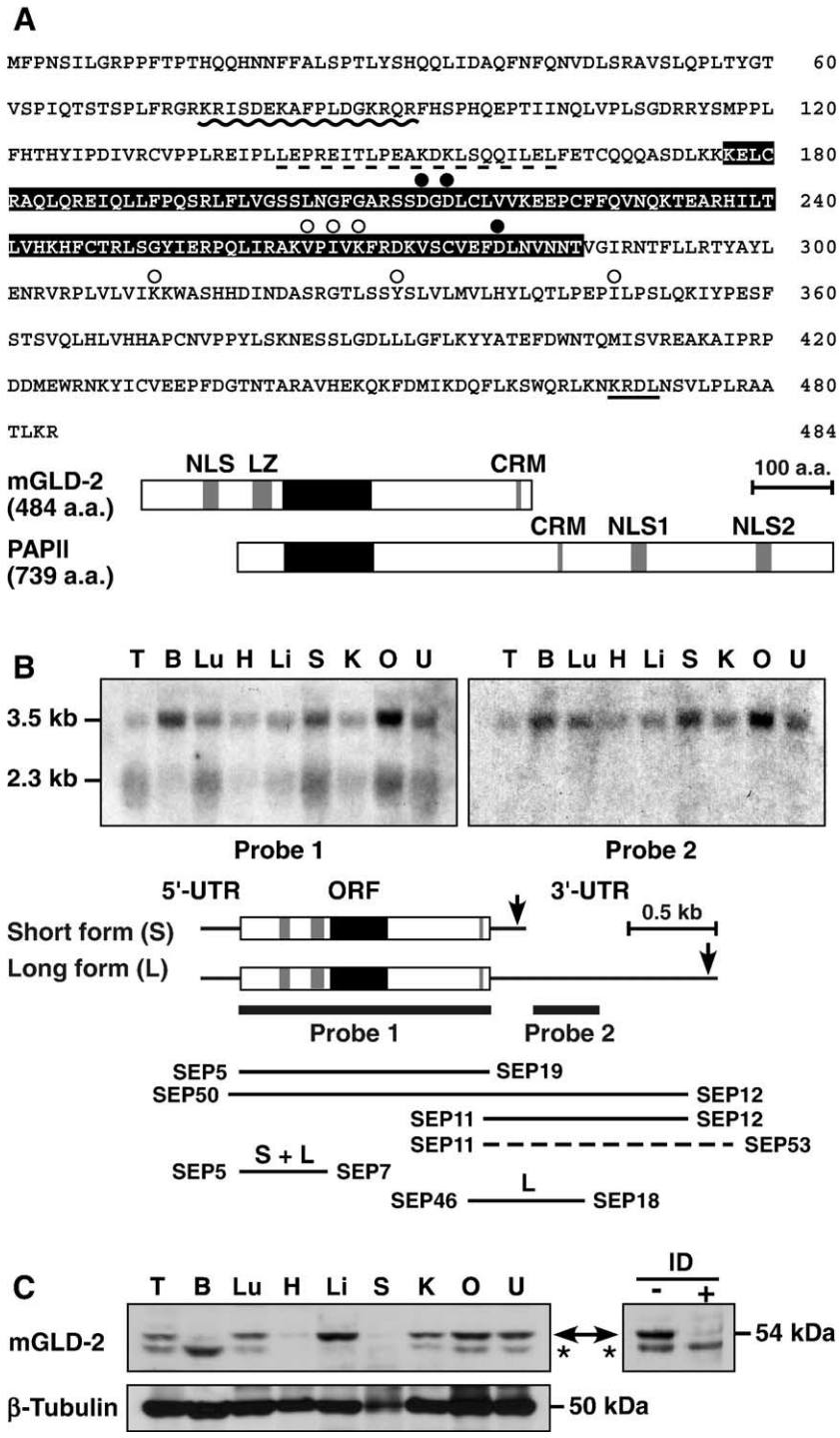

Fig. 1. Protein sequence and expression pattern of mGLD-2. (A) Amino acid sequence and schematic representation of mGLD-2. The putative residues required for binding to two divalent cations and substrate ATP involved in the enzymatic catalysis are indicated by closed and open circles, respectively. Other possible elements similar to the consensus sequences of the bipartite nuclear localization signal (NLS), leucine zipper motif (LZ), and cyclin-recognition motif (CRM) are underlined with wavy, broken, and solid lines, respectively. Note that mGLD-2 lacks an approximately 330-residue C-terminal sequence of mouse PAPII containing the RNA-binding and Ser/Thr-rich domains, and two bipartite nuclear localization signals (NLS1 and NLS2). (B) Northern blot analysis and sequence analysis of two mGLD-2 mRNAs. Total cellular RNAs of testis (T), brain (B), lung (Lu), heart (H), liver (Li), spleen (S), kidney (K), ovary (O), and uterus (U) from adult mice were separated by agarose gel electrophoresis, blotted, and hybridized to ^{32}P-labeled DNA fragment corresponding to probe 1 or probe 2. Three DNA fragments were PCR-amplified from a mouse testicular cDNA library using SEP5/SEP19, SEP50/SEP12, and SEP11/SEP12 primer sets and then sequenced. No DNA fragment was amplified when a SEP11/SEP53 primer set was used. The regions amplified by SEP5/SEP7 and SEP46/SEP18 primer sets, which are common to both short and long forms of mGLD-2 mRNA, and specific for the long form, respectively, are also represented. Arrows indicate the location of putative polyadenylation signals. 5′UTR, 5′untranslated region; ORF, open-reading frame; 3′UTR, 3′untranslated region. (C) Immunoblot analysis. Protein extracts (10 μg) of mouse tissues were separated by SDS-PAGE, blotted, and probed by affinity-purified anti-mGLD-2 or anti-β-tubulin antibody. Asterisks indicate the location of a 51-kDa protein nonspecifically immunoreactive with the anti-mGLD-2 antibody. The 54-kDa mGLD-2 protein was immunodepleted (ID) from the ovarian extracts by treatment with (+) or without (−) antibody against the N-terminal 99-residue polypeptide of mGLD-2, and the resulting supernatant was subjected to immunoblot analysis using affinity-purified anti-mGLD-2 antibody, as described above.

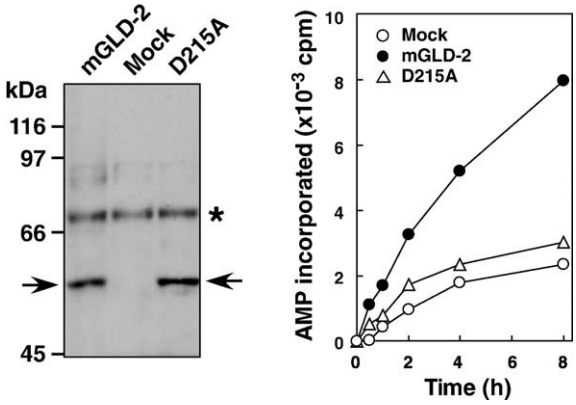

Fig. 2. Polyadenylation activity of mGLD-2 and its mutant D215A. Recombinant proteins fused to FLAG/HA tag (arrows) were produced by an in vitro transcription/translation system and subjected to immunoblot analysis using anti-FLAG antibody as a probe. An asterisk indicates the location of a nonspecific protein band. The enzyme activities of mGLD-2 (closed circle), D215A (open triangle), and mock (open circle) were monitored by measuring the incorporation of AMP from [α-^{32}P]ATP into oligo(A)$_{12}$ primer.

poly(A) tail of the short form of mGLD-2 mRNA at the metaphase-I stage was approximately 100 nucleotides longer than those at other stages of oocyte maturation (Fig. 4B). No significant band was detectable in the long form of mGLD-2 mRNA. Despite the presence of mGLD-2 mRNA (Fig. 4A), the protein level of mGLD-2 was negligibly low both in the oocytes at the GV stage and in those undergoing GVBD (Fig. 4C). The metaphase-I oocytes contained only a low level of mGLD-2, and this protein reached the highest level in the metaphase II-arrested oocytes. These results demonstrate that the short form of mGLD-2 mRNA is predominantly present in the oocytes throughout meiotic maturation, and suggest that the additional extension of the poly(A) tail of mGLD-2 mRNA may be responsible for the protein synthesis during the progress of oocytes from the metaphase I to metaphase II.

To examine the subcellular localization of mGLD-2 in the oocyte, we carried out immunohistochemical analysis using affinity-purified anti-mGLD-2 antibody. However, no rigid data were obtained presumably owing to the low abundance of mGLD-2 (data not shown). Consequently, polyadenylated RNA (0.2 mg/ml) encoding mGLD-2 fused to a FLAG/HA tag at the N-terminus was microinjected into GV-stage oocytes in the presence of dbcAMP, an inhibitor for spontaneous oocyte maturation. Following meiotic maturation of the oocytes in the absence of dbcAMP, the distribution of FLAG/HA-tagged mGLD-2 produced was investigated by immunohistochemical analysis using anti-HA antibody (Fig. 4D). FLAG/HA-tagged mGLD-2 was enriched in the nucleus of the GV-stage oocyte

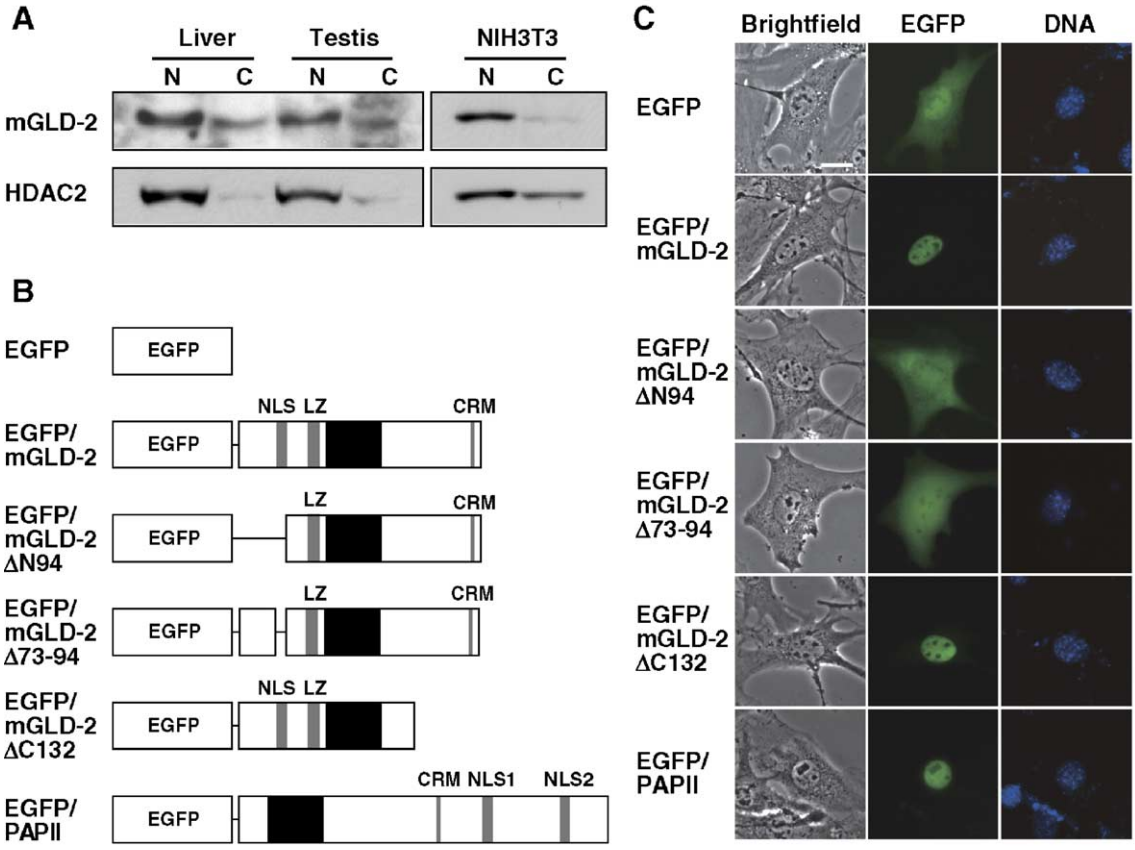

Fig. 3. Localization of mGLD-2 in somatic, testicular, and cultured cells. (A) Immunoblot analysis. Nuclear (N) and cytoplasmic (C) proteins (5 μg) of liver, testis, and NIH3T3 cells were separated by SDS-PAGE, blotted, and probed by anti-mGLD-2 or anti-HDAC2 antibody. (B) Schematic representation of fusion proteins between EGFP and mGLD-2, PAPII, or three mGLD-2 mutants (ΔN94, Δ73–94, and ΔC132). Putative functional motifs, including a bipartite nuclear localization signal (NLS), are indicated. (C) Microscopic analysis. After transfection of expression plasmids, NIH3T3 cells were stained with Hoechst 33342 and observed under a fluorescent microscope. Scale bar = 20 μm.

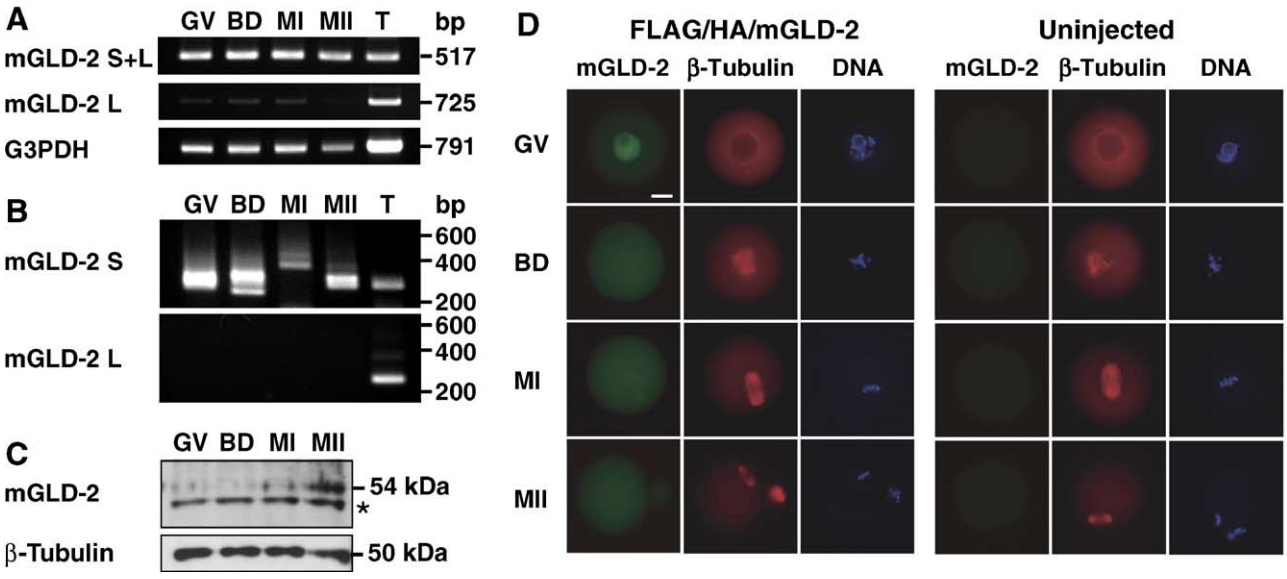

Fig. 4. Delayed synthesis of mGLD-2 during oocyte maturation. (A) RT-PCR analysis. First-strand cDNA was synthesized from total RNA of oocytes at germinal vesicle (GV), GV breakdown (BD), metaphase-I stage (MI), and metaphase-II (MII) stage, and testicular tissues (T). DNA fragments were amplified by RT-PCR from the short (S) and long (L) forms of mGLD-2 mRNA (Fig. 1B) and mRNA for glyceraldehyde-3-phosphate dehydrogenase (G3PDH), as described in the Materials and methods section. (B) PAT assay. The sizes of poly(A) tails of two mGLD-2 mRNAs were measured by PAT assays using total RNA from GV-, BD-, MI-, and MII-stage oocytes and testicular tissues. (C) Immunoblot analysis. Proteins of GV-, BD-, MI-, and MII-stage oocytes (usually 50 cells per lane) were separated by SDS-PAGE, blotted, and probed by affinity-purified anti-mGLD-2 or anti-β-tubulin antibody. An asterisk indicates the location of a 51-kDa protein nonspecifically immunoreactive with the anti-mGLD-2 antibody. (D) Microinjection of polyadenylated RNA. Polyadenylated RNA (0.2 mg/ml) encoding mGLD-2 fused to a FLAG/HA tag was microinjected into GV-stage oocytes. The oocytes were cultured for 6 h in the presence of dbcAMP and underwent spontaneous meiotic maturation in the absence of dbcAMP. At various maturation stages indicated, the oocytes were fixed and immunostained with anti-HA and anti-β-tubulin antibodies. The cell nuclei were also stained with Hoechst 33342. Scale bar = 20 μm.

and was then spread through the cytoplasm following GVBD. These data suggest the cytoplasmic localization of mGLD-2 in the oocytes at metaphases I and II. Moreover, mGLD-2 may be present in the nucleus as well as in the cytoplasm of the GV and GVBD oocytes if the protein is indeed synthesized in these cells (Fig. 4C).

To block translation of mGLD-2 mRNA in oocytes, RNAi was carried out by direct injection of dsRNAs into GV-stage oocytes in the presence of dbcAMP. The reason why we used long dsRNAs for RNAi was because mouse oocytes lack the protein kinase PKR-mediated apoptotic response elicited by long dsRNA in somatic cells (Svoboda et al., 2000; Yu et al., 2004). A dsRNA, termed dsRNAi-1, homologous to the protein-coding region of mGLD-2 was designed to target endogenous mRNA destruction (Fig. 5A). We microinjected dsRNAi-1 or a control dsRNA (dsRNAi-c) matching mouse Mos cDNA (Fig. 5B). mGLD-2 and Mos mRNAs in the GV stage-arrested oocytes in the presence of dbcAMP were analyzed by RT-PCR 20 h after dsRNA injection (Fig. 5C). The injections of dsRNAi-1 and dsRNAi-c showed approximately 62 and 75% reduction of mGLD-2 and Mos mRNAs after the 20-h culture, relative to negative controls (oocytes without dsRNA injection), respectively (arrows in Fig. 5C). Moreover, the injection of mGLD-2 and Mos sense RNA (sRNAi-1 and sRNAi-c, respectively) had no significant effect on the level of the endogenous mRNA.

GV-stage oocytes, which had been injected with dsRNAi-1 or dsRNAi-c, were then cultured in vitro in the absence of dbcAMP to undergo spontaneous meiotic maturation (Fig. 5B). GVBD was observed in most oocytes (approximately 95%) 2–3 h after culture. As compared with oocytes without dsRNA injection, the dsRNAi-1-injected oocytes revealed a significant delay in meiotic maturation; 36% of total oocytes were arrested or remained at metaphase I even after 18-h culture (Fig. 5D), despite normal spindle formation (data not shown). RT-PCR analysis indicated that the levels of mGLD-2 mRNA in the metaphase-I and metaphase-II oocytes previously injected with dsRNAi-1 are 24 and 2% of those without dsRNA injection, respectively (arrows in Fig. 5E). Consistent with the fact that Mos is involved in the maintenance of the metaphase-II arrest (Colledge et al., 1994; Hashimoto et al., 1994; Wianny and Zernicka-Goetz, 2000), 21% of total oocytes injected with dsRNAi-c progressed to one-cell embryos with a single pronucleus due to spontaneous parthenogenetic activation (Fig. 5D). These data suggest that mGLD-2 may play an important role in the progression of metaphase I to metaphase II during oocyte maturation.

Mouse oocytes barely contain mGLD-2 at GV and GVBD stages of meiotic maturation (Fig. 4C), as described above. To examine whether overproduction of mGLD-2 affects oocyte maturation, we microinjected polyadenylated mGLD-2 RNA into GV-stage oocytes, using polyadenylated RNAs of mutant protein D215A and EGFP as controls (Fig. 6A). When the oocytes were cultured in the presence of dbcAMP for 6 h and then underwent spontaneous maturation in the absence of dbcAMP, the mGLD-2 RNA (1.0 mg/ml)-injected oocytes were mostly (88%) arrested at metaphase I after 18-h culture (Fig. 6B). The oocytes injected with polyadenylated D215A or

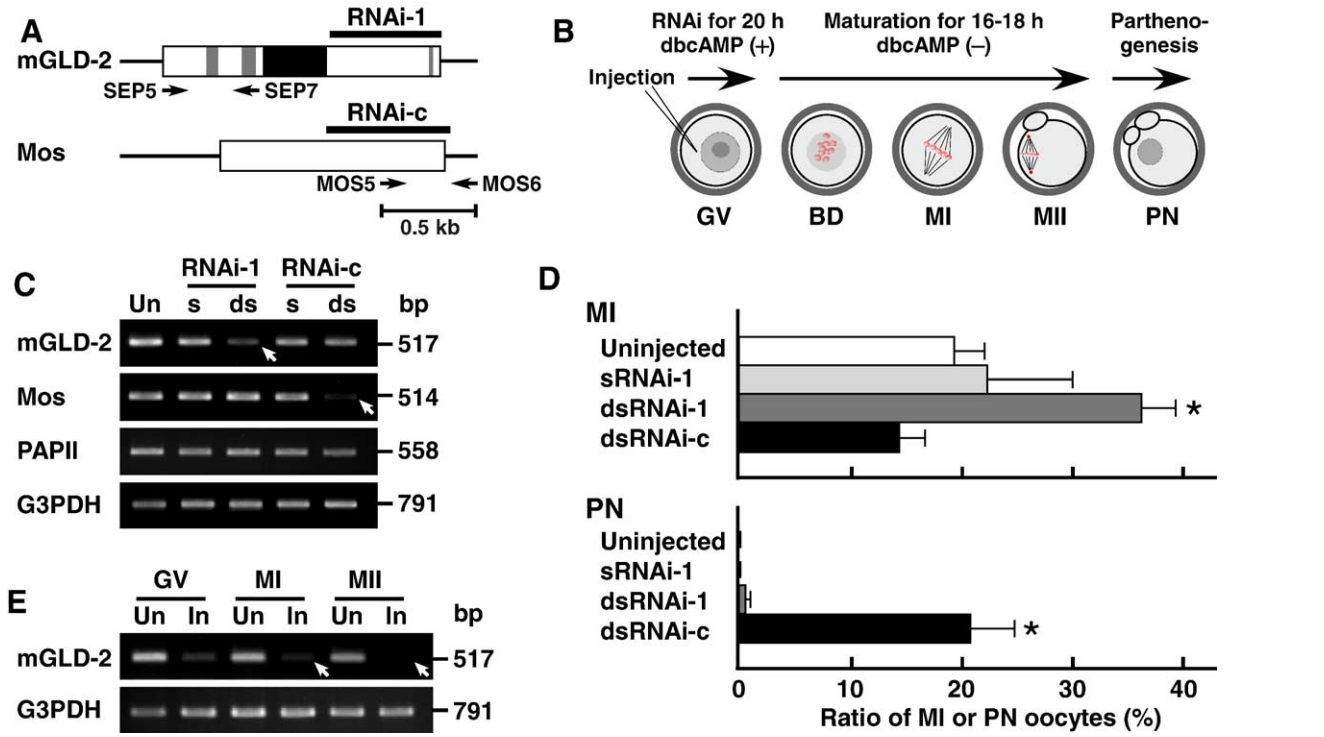

Fig. 5. Arrest of oocyte maturation by impaired synthesis of mGLD-2. (A) Targeted regions for endogenous mRNA destruction. Two dsRNAs, dsRNAi-1 and dsRNAi-c, homologous to the protein-coding and 3′-untranslated regions of mGLD-2 and Mos, respectively, were designed to target endogenous mRNA destruction. Single-strand sense RNAs (sRNAi-1 and sRNAi-c) covering the same regions were also synthesized in vitro. Arrows indicate the location of oligonucleotide primers used for RT-PCR. (B) Schematic diagram of the procedures for RNAi. Germinal vesicle (GV)-stage oocytes were injected with sRNA or dsRNA, incubated in the presence of dbcAMP for 20 h, cultured in the absence of dbcAMP for 16–18 h, and stained with Hoechst 33342. The GV breakdown (BD)-, metaphase I (MI)-, metaphase II (MII)-, and pronuclear (PN)-stage oocytes were then observed microscopically. (C) Specific reduction of endogenous mRNA in GV-stage oocytes by RNAi. After injection of sRNA (s) or dsRNA (ds), the GV-stage oocytes were incubated for 20 h in the presence of dbcAMP and then subjected to RT-PCR analysis using uninjected oocytes (Un) as a control. Arrows indicate the reduction of mGLD-2 and Mos mRNAs. (D) Arrest of oocyte maturation at the MI stage. After culture in the absence of dbcAMP, the stages of oocyte maturation were microscopically assessed. The oocytes injected with sRNA or dsRNA at the GV-stage still remained at the GV stage, developed into the MI-, MII-, and PN-stage oocytes, or caused fragmentation (approximately 10% of total oocytes). The relative ratios of the MI- and PN-stage oocytes to total oocytes injected with sRNA or dsRNA are expressed as the means ± SE, where $n \geq 3$. Numbers of oocytes examined are as follows: 48, 181, and 94 oocytes for sRNAi-1 ($n = 3$), dsRNAi-1 ($n = 9$), and dsRNAi-c ($n = 8$), respectively. Uninjected oocytes (131 cells, $n = 9$) were used as a control. *Differences between “uninjected” and “dsRNAi-1” and between “uninjected” and “dsRNAi-c” are statistically significant ($P < 0.005$, Student’s t test). (E) Reduction of endogenous mGLD-2 mRNA during oocyte maturation by RNAi. Total RNA was prepared from the GV-, MI-, and MII-stage oocytes previously uninjected (Un) or injected (In) with dsRNAi-1 and subjected to RT-PCR analysis as described above. Arrows indicate the reduction of mGLD-2 mRNA in the MI- and MII-stage oocytes.

EGFP RNA (1.0 mg/ml) normally underwent meiotic maturation. Thus, overproduction of mGLD-2 also prevents the oocytes from progressing from metaphase I to metaphase II.

Some mRNAs, including those of cyclin B1, Mos, and β-catenin, are known to be polyadenylated during oocyte maturation (Gebauer et al., 1994; Oh et al., 2000; Tay et al., 2000). To ascertain the effects of enhanced production of mGLD-2 on the poly(A) tails of these three mRNAs, PAT assays for polyadenylated RNA-injected oocytes were carried out (Fig. 6C). The poly(A) tails of cyclin B1, Mos, and β-catenin mRNAs in the GV-arrested oocytes injected with polyadenylated mGLD-2 RNA were approximately 50–100 nucleotides longer than those in the oocytes uninjected and injected with polyadenylated D215A RNA. No significant difference of the poly(A) tail in length was found at the metaphase-I stage among the uninjected and polyadenylated mGLD-2 and D215A RNA-injected oocytes. Thus, the overproduction of mGLD-2 in the GV-stage oocytes results in the additional poly(A) elongation of at least cyclin B1, Mos, and β-catenin mRNAs, suggesting that the artificial, unnecessary extension of mRNA poly(A) tails at the GV stage may be implicated in the metaphase-I arrest of oocytes.

Discussion

This study describes the nuclear and cytoplasmic localization of mGLD-2 in somatic, testicular, and cultured cells. Transient expression analysis of EGFP/mGLD-2 chimeric proteins in NIH3T3 cells demonstrates that the region required for guiding mGLD-2 to the nucleus is present within the 22-residue sequence containing a putative bipartite NLS at residues 76–92 (Figs. 1 and 3). Although mGLD-2 is also capable of residing in the nucleus of the GV-stage oocytes, the mouse oocytes have a specialized program for mGLD-2 in which its mRNA is effectively translated after GVBD during oocyte maturation (Fig. 4). Both artificial impairment and enhancement of mGLD-2 synthesis lead to the arrest of oocyte maturation at the metaphase-I stage (Figs. 5 and 6). Thus, in the

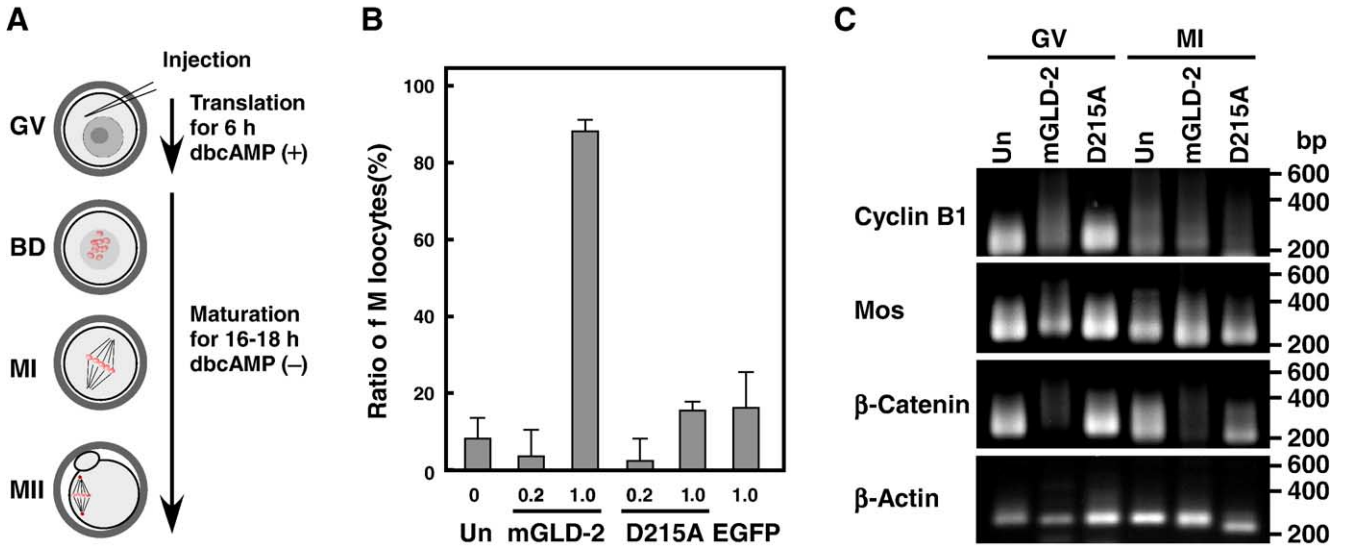

Fig. 6. Arrest of oocyte maturation by overproduction of mGLD-2. (A) Schematic diagram of the procedures for mGLD-2 overproduction. Germinal vesicle (GV)-stage oocytes were injected with polyadenylated RNA, incubated in the presence of dbcAMP for 6 h, cultured in the absence of dbcAMP for 16–18 h, and stained with Hoechst 33342. The stages of oocyte maturation were then assessed microscopically. (B) Arrest of oocyte maturation at the MI stage. After culture in the absence of dbcAMP, the maturation stages of oocytes previously injected with polyadenylated RNA (0.2 or 1.0 mg/ml) were assessed. Data are expressed as the means ± SE, where $n \geq 3$. Numbers of oocytes examined are as follows: 42, 89, 40, and 91 oocytes for polyadenylated RNAs of 0.2 mg/ml mGLD-2 ($n = 3$), 1.0 mg/ml mGLD-2 ($n = 5$), 0.2 mg/ml D215A ($n = 3$, see Fig. 2), and 1.0 mg/ml D215A ($n = 6$), respectively. Oocytes previously uninjected (78 cells, $n = 4$) or injected with 1.0 mg/ml EGFP (35 cells, $n = 3$) were used as controls. Note that all oocytes underwent GVBD and were arrested at the MI or MII stage after culture in the absence of dbcAMP for 16–18 h. (C) PAT assay. GV-stage oocytes were injected with and without (Un) polyadenylated RNA, incubated in the presence of dbcAMP for 6 h, and cultured in the absence of dbcAMP for 7 h (MI-stage oocytes). The sizes of poly(A) tails of cyclin B1, Mos, β-catenin, and β-actin as a negative control were measured by PAT assays using total RNA from the GV- and MI-stage oocytes. Note that overproduction of mGLD-2 in the GV-stage oocytes results in the additional poly(A) elongation of cyclin B1, Mos, and β-catenin mRNAs.

mouse oocytes, mGLD-2 as well as the *C. elegans* and *Xenopus* proteins presumably participates in cytoplasmic polyadenylation of a subset of pre-existing mRNAs essential for the meiotic maturation.

Computer-aided search on the PROSITE database of protein families and domains indicates that the sequences of *C. elegans* and *Xenopus* GLD-2 contain a single set of potential bipartite NLS at residues 1071–1087 and 99–115 (or 100–116) in the C- and N-terminal regions, respectively (data not shown). These two GLD-2 proteins have been shown to localize in the cytoplasm of embryos and cultured cells (Barnard et al., 2004; Wang et al., 2002), although *Xenopus* GLD-2 is both cytoplasmic and nuclear in the stage-VI oocytes (Rouhana et al., 2005). Our data represented in this study demonstrate the presence of mGLD-2 in the cytoplasm of mouse oocytes at metaphases I and II (Fig. 4). However, the subcellular destination of mGLD-2 to the ooplasm results from the translational control of the mGLD-2 mRNA. Indeed, mGLD-2 is enriched in the nucleus when polyadenylated mGLD-2 RNA is injected into mouse oocytes at the GV (Fig. 4) and pronuclear stages (data not shown). Because *Xenopus* GLD-2 resides in a protein complex of cytoplasmic polyadenylation machinery even in the oocytes prior to GVBD (Barnard et al., 2004), the functional role of mGLD-2 during oocyte maturation may be similar to but distinguishable from that of *Xenopus* GLD-2.

The presence of mGLD-2 in the cell nucleus (Fig. 3) is intriguing since this protein contains a putative CRM sequence, Lys–Arg–Asp–Leu, at the position similar to that of PAPII (Fig. 1). The CRM of canonical nuclear PAP (PAPI and PAPII) is shown to interact with both G_1- and G_2-type cyclins and mediate phosphorylation of PAP by cyclin-dependent kinases (Bond et al., 2000). Furthermore, the PAP hyperphosphorylation during mitosis and oocyte maturation results in the loss of the polyadenylation activity (Colgan et al., 1998). It is thus conceivable that the maintenance of normal level of PAP phosphorylation is probably mediated via the CRM throughout the cell cycle and that the inhibition of PAP may prevent incorrect lengthening of mRNA poly(A) tails in the cytoplasm of M-phase cells (Bond et al., 2000; Colgan et al., 1998). Our preliminary experiments have indicated that the molecular mass of mGLD-2 exogenously expressed by injection of the polyadenylated RNA is approximately 1 kDa higher in the cytoplasm of the metaphase-I and -II oocytes than in the nucleus of the GV-stage oocytes (data not shown), implying possible phosphorylation of mGLD-2 in the cytoplasm of the metaphase oocytes. Even so, mGLD-2 must be functionally active, as described in Figs. 5 and 6. Thus, the regulation of the polyadenylation activity by protein (hyper)phosphorylation may be different between mGLD-2 and canonical PAP in the oocytes.

Translational activation of mRNAs in the cytoplasm of oocytes is basically coupled with their polyadenylation (Richter, 2000). In the present study, the poly(A) tail of mGLD-2 mRNA is elongated at the metaphase-I stage and then deadenylated at the metaphase-II stage of mouse oocytes (Fig. 4B). However, mGLD-2 synthesis occurs in the metaphase-I oocytes at a detectable level, and the protein is accumulated at

the maximum level in the metaphase-II oocytes (Fig. 4C). There is an apparent discrepancy in the time between poly(A) tail lengthening and protein synthesis. The delayed synthesis of mGLD-2 may be explained by a possible continuation of the poly(A) tail lengthening or maintenance of the elongated poly(A) tail during the oocyte transition from the metaphase-I to metaphase-II stages. Indeed, the GVBD, metaphase-I, and metaphase-II oocytes are recovered 2–3, 7–8, and 16–18 h after culture of the GV-stage oocytes in the absence of dbcAMP (Fig. 5B), respectively, and are analyzed by RT-PCR and immunoblotting (Figs. 5B and C). If the above possibility is correct, mGLD-2 is probably accumulated in the oocytes until the metaphase-II stage.

The precise translational control of mGLD-2 is essential for oocyte maturation because meiotic maturation is inhibited or delayed by both knockdown and overproduction of mGLD-2 in the GV-stage oocytes (Figs. 5 and 6). The overproduction leads to aberrant polyadenylation of cyclin B1, Mos, and β-catenin mRNAs at the GV stage (Fig. 6C). Then, translational activation of these three mRNAs may occur, which results in the metaphase-I arrest of the oocytes (Fig. 6B). In some experiments, we examined the effects of RNAi-induced knockdown of mGLD-2 on poly(A) tail lengths of the above mRNAs at the GV and metaphase-I stages. Although poly(A) tail lengthening was expected to be defective in the mGLD-2-knockdown oocytes, the poly(A) tails of cyclin B1, Mos, and β-catenin mRNAs were apparently elongated normally at the metaphase-I stage (data not shown). A possible reason for the unexpected results is because more than 20% of mGLD-2 mRNA still remain in the metaphase-I oocytes after dsRNA-1 injection (Fig. 5E). A small amount of mGLD-2 appears to be synthesized in the metaphase-I oocytes, which may be implicated in the delay in meiotic maturation (Fig. 5D). Another reason may be due to the sensitivity of PAT assay. Despite a low abundance, an elongated mRNA poly(A) tail can be amplified by this assay system. Thus, further experiments remain necessary to clarify the effects of mGLD-2 knockdown on poly(A) tail lengthening in the metaphase-I oocytes.

As described above, the accumulation of mGLD-2 in the oocytes starts at the time when the poly(A) tail lengthening of mGLD-2 mRNA occurs (Fig. 4). Despite the presence of mGLD-2 mRNA, the protein level is negligibly low in the GV and GVBD oocytes, suggesting that this mRNA is most likely under translational control during oocyte maturation. Thus, the oocytes appear to require the precise translation of mGLD-2 mRNA during the transition from metaphase I to metaphase II. This probability may be supported by the fact that both knockdown and overproduction of mGLD-2 result in the arrest and/or delay of oocyte maturation at the metaphase-I stage.

On the basis of the interaction of GLD-2 with known polyadenylation factors, at least two distinct polyadenylation complexes, G and MP complexes, have been proposed to exist in the cytoplasm of *Xenopus* stage-VI oocytes (Barnard et al., 2004; Rouhana et al., 2005). GLD-2 is included in the G-complex together with CPEB, CPSF, and possibly symplekin, whereas the MP complex contains CPEB, maskin, and Pumilio. Rouhana et al. (2005) suggest that actively and inactively translated mRNAs may be partitioned between the G and MP complexes during oocyte maturation. In the mouse brain, mGLD-2 mRNA is shown to co-localize with those of CPEB and Pumilio presumably involved in synaptic plasticity, implying an importance of mGLD-2 in the translational activation at synapses (Rouhana et al., 2005). Our data show that meiotic maturation of the mouse oocytes requires the precise translational control of mGLD-2 (Figs. 5 and 6), as described above. The low abundance or absence of this enzyme at the GV and GVBD stages seems to prevent the substrate mRNAs from starting the polyadenylation-induced translation. We thus suggest that mGLD-2 may act as a positive regulator in the progression of metaphase I to metaphase II during oocyte maturation.

It has been reported that CPEB, CPSF100, and maskin as the components of the G and MP complexes are present in the GV- through metaphase II-stage mouse oocytes (Hodgman et al., 2001). Because maskin is known to interact with translationally repressed mRNAs (Richter, 2000), cytoplasmic polyadenylation in the oocytes may be conducted by mGLD-2 in the G complex at the metaphases I and II, together with maskin-mediated repression. This coordinated regulation of mRNA poly(A) tails may help to ensure the progression of oocyte maturation. Nevertheless, the substrate mRNAs for mGLD-2 in the G complex remain to be identified. Some of the mRNA targets of oocyte mGLD-2 are possibly mRNAs encoding regulatory proteins involved in the cell cycle progression and the organization of spindles and microfilaments, including CKS2 (Spruck et al., 2003) and formin-2 (Leader et al., 2002). Indeed, mutant mice lacking CKS2 or formin-2 show the oocyte arrest at the metaphase-I stage.

Targeting of *C. elegans* GLD-2 to specific mRNAs is probably regulated by the binding partner GLD-3 because GLD-3 belongs to a Bicaudal-C family of RNA-binding proteins (Wang et al., 2002; Wessely et al., 2001). In *Xenopus* GLD-2, CPEB, CPSF, and possibly symplekin in the cytoplasmic polyadenylation machinery likely direct GLD-2 to recruit to specific mRNAs containing the CPE signal (Barnard et al., 2004). Thus, to elucidate the functional role(s) of mGLD-2, both the post-translational modification of mGLD-2 and the interaction of this protein with other unknown proteins remain to be examined. The leucine zipper motif present in mGLD-2 may help to know a possible interaction(s) with regulatory proteins, DNA, and/or RNA.

Acknowledgments

This study was partly supported by Grant-in-Aids for Scientific Research on Priority Areas, Scientific Researches (A) and (B), Young Scientists (B), and Exploratory Research from Japan Society for the Promotion of Science (JSPS) and Ministry of Education, Culture, Sports, Science and Technology in Japan (MEXT), and by the 21st Century COE Program from MEXT.

References

Barnard, D.C., Ryan, K., Manley, J.L., Richter, J.D., 2004. Symplekin and xGLD-2 are required for CPEB-mediated cytoplasmic polyadenylation. Cell 119, 641–651.

Bilger, A., Fox, C.A., Wahle, E., Wickens, M., 1994. Nuclear polyadenylation factors recognize cytoplasmic polyadenylation elements. Genes Dev. 8, 1106–1116.

Bond, G.L., Prives, C., Manley, J.L., 2000. Poly(A) polymerase phosphorylation is dependent on novel interactions with cyclins. Mol. Cell. Biol. 20, 5310–5320.

Cao, Q., Richter, J.D., 2002. Dissolution of the maskin–eIF4E complex by cytoplasmic polyadenylation and poly(A)-binding protein controls cyclin B1 mRNA translation and oocyte maturation. EMBO J. 21, 3852–3862.

Colgan, D.F., Murthy, K.G., Zhao, W., Prives, C., Manley, J.L., 1998. Inhibition of poly(A) polymerase requires p34cdc2/cyclin B phosphorylation of multiple consensus and non-consensus sites. EMBO J. 17, 1053–1062.

Colledge, W.H., Carlton, M.B., Udy, G.B., Evans, M.J., 1994. Disruption of c-*mos* causes parthenogenetic development of unfertilized mouse eggs. Nature 370, 65–68.

Dickson, K.S., Bilger, A., Ballantyne, S., Wickens, M.P., 1999. The cleavage and polyadenylation specificity factor in *Xenopus laevis* oocytes is a cytoplasmic factor involved in regulated polyadenylation. Mol. Cell. Biol. 19, 5707–5717.

Gebauer, F., Xu, W., Cooper, G.M., Richter, J.D., 1994. Translational control by cytoplasmic polyadenylation of *c-mos* mRNA is necessary for oocyte maturation in the mouse. EMBO J. 13, 5712–5720.

Hake, L.E., Mendez, R., Richter, J.D., 1998. Specificity of RNA binding by CPEB: requirement for RNA recognition motifs and a novel zinc finger. Mol. Cell. Biol. 18, 685–693.

Hashimoto, N., Watanabe, N., Furuta, Y., Tamemoto, H., Sagata, N., Yokoyama, M., Okazaki, K., Nagayoshi, M., Takeda, N., Ikawa, Y., Aizawa, S., 1994. Parthenogenetic activation of oocytes in *c-mos*-deficient mice. Nature 370, 68–71.

Hodgman, R., Tay, J., Mendez, R., Richter, J.D., 2001. CPEB phosphorylation and cytoplasmic polyadenylation are catalyzed by the kinase IAK1/Eg2 in maturing mouse oocytes. Development 128, 2815–2822.

Honda, A., Yamagata, K., Sugiura, S., Watanabe, K., Baba, T., 2002. A mouse serine protease TESP5 is selectively included into lipid rafts of sperm membrane presumably as a glycosylphosphatidylinositol-anchored protein. J. Biol. Chem. 277, 16976–16984.

Kadyk, L.C., Kimble, J., 1998. Genetic regulation of entry into meiosis in *Caenorhabditis elegans*. Development 125, 1803–1813.

Kashiwabara, S., Baba, T., Takada, M., Watanabe, K., Yano, Y., Arai, Y., 1990. Primary structure of mouse proacrosin deduced from the cDNA sequence and its gene expression during spermatogenesis. J. Biochem. 108, 785–791.

Kashiwabara, S., Zhuang, T., Yamagata, K., Noguchi, J., Fukamizu, A., Baba, T., 2000. Identification of a novel isoform of poly(A) polymerase, TPAP, specifically present in the cytoplasm of spermatogenic cells. Dev. Biol. 228, 106–115.

Kashiwabara, S., Noguchi, J., Zhuang, T., Ohmura, K., Honda, A., Sugiura, S., Miyamoto, K., Takahashi, S., Inoue, K., Ogura, A., Baba, T., 2002. Regulation of spermatogenesis by testis-specific, cytoplasmic poly(A) polymerase TPAP. Science 298, 1999–2002.

Kim, E., Nishimura, H., Iwase, S., Yamagata, K., Kashiwabara, S., Baba, T., 2004. Synthesis, processing, and subcellular localization of mouse ADAM3 during spermatogenesis and epididymal sperm transport. J. Reprod. Dev. 50, 571–578.

Kuersten, S., Goodwin, E.B., 2003. The power of the 3′ UTR: translational control and development. Nat. Rev., Genet. 4, 626–637.

Kwak, J.E., Wang, L., Ballantyne, S., Kimble, J., Wickens, M., 2004. Mammalian GLD-2 homologs are poly(A) polymerases. Proc. Natl. Acad. Sci. U. S. A. 101, 4407–4412.

Kyriakopoulou, C.B., Nordvarg, H., Virtanen, A., 2001. A novel nuclear human poly(A) polymerase (PAP), PAPγ. J. Biol. Chem. 276, 33504–33511.

Leader, B., Lim, H., Carabatsos, M.J., Harrington, A., Ecsedy, J., Pellman, D., Maas, R., Leder, P., 2002. Formin-2, polyploidy, hypofertility and positioning of the meiotic spindle in mouse oocytes. Nat. Cell Biol. 4, 921–928.

Martin, G., Keller, W., Doublie, S., 2000. Crystal structure of mammalian poly(A) polymerase in complex with an analog of ATP. EMBO J. 19, 4193–4203.

Martin, G., Moglich, A., Keller, W., Doublie, S., 2004. Biochemical and structural insights into substrate binding and catalytic mechanism of mammalian poly(A) polymerase. J. Mol. Biol. 341, 911–925.

Mendez, R., Richter, J.D., 2001. Translational control by CPEB: a means to the end. Nat. Rev., Mol. Cell Biol. 2, 521–529.

Nishimura, H., Kim, E., Nakanishi, T., Baba, T., 2004. Possible function of the ADAM1a/ADAM2 Fertilin complex in the appearance of ADAM3 on the sperm surface. J. Biol. Chem. 279, 34957–34962.

Oh, B., Hwang, S., McLaughlin, J., Solter, D., Knowles, B.B., 2000. Timely translation during the mouse oocyte-to-embryo transition. Development 127, 3795–3803.

Ohmura, K., Kohno, N., Kobayashi, Y., Yamagata, K., Sato, S., Kashiwabara, S., Baba, T., 1999. A homologue of pancreatic trypsin is localized in the acrosome of mammalian sperm and is released during acrosome reaction. J. Biol. Chem. 274, 29426–29432.

Raabe, T., Bollum, F.J., Manley, J.L., 1991. Primary structure and expression of bovine poly(A) polymerase. Nature 353, 229–234.

Raabe, T., Murthy, K.G., Manley, J.L., 1994. Poly(A) polymerase contains multiple functional domains. Mol. Cell. Biol. 14, 2946–2957.

Rassa, J.C., Wilson, G.M., Brewer, G.A., Parks, G.D., 2000. Spacing constraints on reinitiation of paramyxovirus transcription: the gene end U tract acts as a spacer to separate gene end from gene start sites. Virology 274, 438–449.

Read, R.L., Martinho, R.G., Wang, S.W., Carr, A.M., Norbury, C.J., 2002. Cytoplasmic poly(A) polymerases mediate cellular responses to S phase arrest. Proc. Natl. Acad. Sci. U. S. A. 99, 12079–12084.

Richter, J.D., 1999. Cytoplasmic polyadenylation in development and beyond. Microbiol. Mol. Biol. Rev. 63, 446–456.

Richter, J.D., 2000. Influence of polyadenylation-induced translation on metazoan development and neuronal synaptic plasticity. In: Sonenberg, N., Herchey, J., Mathews, M.B. (Eds.), Translational Control of Gene Expression. Cold Spring Harbor Laboratory Press, New York, pp. 785–805.

Rouhana, L., Wang, L., Buter, N., Kwak, J.E., Schiltz, C.A., Gonzalez, T., Kelley, A.E., Landry, C.F., Wickens, M., 2005. Vertebrate GLD2 poly(A) polymerases in the germline and the brain. RNA 11, 1117–1130.

Sachs, A.B., Sarnow, P., Hentze, M.W., 1997. Starting at the beginning, middle, and end: translation initiation in eukaryotes. Cell 89, 831–838.

Saitoh, S., Chabes, A., McDonald, W.H., Thelander, L., Yates, J.R., Russell, P., 2002. Cid13 is a cytoplasmic poly(A) polymerase that regulates ribonucleotide reductase mRNA. Cell 109, 563–573.

Schultz, R.M., Montgomery, R.R., Belanoff, J.R., 1983. Regulation of mouse oocyte meiotic maturation: implication of a decrease in oocyte cAMP and protein dephosphorylation in commitment to resume meiosis. Dev. Biol. 97, 264–273.

Sheets, M.D., Wu, M., Wickens, M., 1995. Polyadenylation of c-mos mRNA as a control point in *Xenopus* meiotic maturation. Nature 374, 511–516.

Spruck, C.H., de Miguel, M.P., Smith, A.P., Ryan, A., Stein, P., Schultz, R.M., Lincoln, A.J., Donovan, P.J., Reed, S.I., 2003. Requirement of Cks2 for the first metaphase/anaphase transition of mammalian meiosis. Science 300, 647–650.

Stebbins-Boaz, B., Cao, Q., de Moor, C.H., Mendez, R., Richter, J.D., 1999. Maskin is a CPEB-associated factor that transiently interacts with elF-4E. Mol. Cell 4, 1017–1027.

Svoboda, P., Stein, P., Hayashi, H., Schultz, R.M., 2000. Selective reduction of dormant maternal mRNAs in mouse oocytes by RNA interference. Development 127, 4147–4156.

Tay, J., Hodgman, R., Richter, J.D., 2000. The control of cyclin B1 mRNA translation during mouse oocyte maturation. Dev. Biol. 221, 1–9.

Thuresson, A.C., Astrom, J., Astrom, A., Gronvik, K.O., Virtanen, A., 1994. Multiple forms of poly(A) polymerases in human cells. Proc. Natl. Acad. Sci. U. S. A. 91, 979–983.

Tomecki, R., Dmochowska, A., Gewartowski, K., Dziembowski, A., Stepien, P.P., 2004. Identification of a novel human nuclear-encoded mitochondrial poly(A) polymerase. Nucleic Acids Res. 32, 6001–6014.

Topalian, S.L., Kaneko, S., Gonzales, M.I., Bond, G.L., Ward, Y., Manley, J.L., 2001. Identification and functional characterization of neo-poly(A) polymerase, an RNA processing enzyme overexpressed in human tumors. Mol. Cell. Biol. 21, 5614–5623.

Toyoda, Y., Yokoyama, M., Hoshi, T., 1971. Studies on the fertilization of mouse eggs in vitro. Jpn. J. Anim. Reprod. 16, 147–151.

Wahle, E., 1991. Purification and characterization of a mammalian polyadenylate polymerase involved in the 3′ end processing of messenger RNA precursors. J. Biol. Chem. 266, 3131–3139.

Wang, S.W., Toda, T., MacCallum, R., Harris, A.L., Norbury, C., 2000. Cid1, a fission yeast protein required for S-M checkpoint control when DNA polymerase δ or ε is inactivated. Mol. Cell. Biol. 20, 3234–3244.

Wang, L., Eckmann, C.R., Kadyk, L.C., Wickens, M., Kimble, J., 2002. A regulatory cytoplasmic poly(A) polymerase in *Caenorhabditis elegans*. Nature 419, 312–316.

Wessely, O., Tran, U., Zakin, L., De Robertis, E.M., 2001. Identification and expression of the mammalian homologue of *Bicaudal-C*. Mech. Dev. 101, 267–270.

Wianny, F., Zernicka-Goetz, M., 2000. Specific interference with gene function by double-stranded RNA in early mouse development. Nat. Cell Biol. 2, 70–75.

Wickens, M., Anderson, P., Jackson, R.J., 1997. Life and death in the cytoplasm: messages from the 3′ end. Curr. Opin. Genet. Dev. 7, 220–232.

Yu, J., Deng, M., Medvedev, S., Yang, J., Hecht, N.B., Schultz, R.M., 2004. Transgenic RNAi-mediated reduction of MSY2 in mouse oocytes results in reduced fertility. Dev. Biol. 268, 195–206.

Zhao, W., Manley, J.L., 1996. Complex alternative RNA processing generates an unexpected diversity of poly(A) polymerase isoforms. Mol. Cell. Biol. 16, 2378–2386.